

False Data Injection Cyber-Attack Detection

Xingpeng Li, *Student Member, IEEE* and Kory W. Hedman, *Member, IEEE*

Abstract— State estimation estimates the system condition in real-time and provides a base case for other energy management system (EMS) applications including real-time contingency analysis and security-constrained economic dispatch. Recent work in the literature shows malicious cyber-attack can inject false measurements that bypass traditional bad data detection and cause actual overloads. Thus, it is very important to detect such cyber-attacks. In this paper, multiple metrics are proposed to monitor abnormal load deviations and suspicious branch flow changes. A systematic two-stage approach is proposed to detect false data injection (FDI) cyber-attack. The first stage determines whether the system is under attack while the second stage identifies the target branch. Numerical simulations verify that FDI can cause severe system violations and demonstrate the effectiveness of the proposed two-stage FDI detection (FDID) method. It is concluded that the proposed FDID approach can efficiently detect FDI cyber-attacks and identify the target branch; furthermore, the associated false alarm rate and false dismissal rate are very low.

Index Terms—Cyber-attack, false data injection, false data injection detection, power system cyber-security, security-constrained economic dispatch, state estimation.

NOMENCLATURE

Sets

K	Set of branches.
KA	Set of branches that have the top ten values for malicious load deviation index.
$K(n-)$	Set of branches with bus n as from-bus.
$K(n+)$	Set of branches with bus n as to-bus.
N	Set of buses.
NL	Set of load buses.
$NL(k)$	Set of load buses that are critical to branch k .

Indices

k	branch.
n	bus.
$n(k-)$	From-bus of branch k .
$n(k+)$	To-bus of branch k .

Parameters

d_{n0}	Actual load at bus n at $t = 0$.
$d_{n0,M}$	Load measurement at bus n at $t = 0$.
d_{n-}	Actual load at bus n at $t = -T_{ED}$.
l	Target branch l of FDI attack.
L_S	Load shift factor.
$Limit_k$	Thermal limit of branch k .
N_1	Limit of an l_1 -norm constraint.
NL_k	Number of load buses that are critical to branch k .

$P_{l,0}$	Actual flow on target branch l at $t = 0$.
P_{k0}	Actual flow on branch k at $t = 0$.
$P_{k0,M}$	Measurement of flow on branch k at $t = 0$.
P_{k-}	Actual flow on branch k at $t = -T_{ED}$.
$PTDF_{n,k}$	Power transfer distribution factor for branch k due to an injection change at bus n .
T_{ED}	Interval of a SCED period.
x_k	Reactance of branch k .
Δd_n	Actual load difference at bus n between $t = 0$ and $t = -T_{ED}$.

Variables

c	Attack vector of bus phase angles.
$\Delta \tilde{d}_n$	Malicious load deviation at bus n .
p_l	Post-attack actual flow on target branch l .
\tilde{p}_l	Post-attack cyber flow on target branch l .
p_k	Post-attack actual flow on branch k .
\tilde{p}_k	Post-attack cyber flow on branch k .
Δp_l	Difference between the post-attack actual power flow and cyber power flow on the target branch l .
Δp_k	Difference between the post-attack actual power flow and cyber power flow on branch k .
θ_n	Post-attack actual phase angle of bus n .
$\tilde{\theta}_n$	Post-attack cyber phase angle of bus n .

Metrics

ALB_k	Alert level of branch k , associated with $BORI_k$.
ALC_k	Comprehensive alert level of branch k .
ALE_k	Alert level of branch k , associated with $EMLDI_k$.
$BORI_k$	Branch overload risk index of branch k .
CI_k	Comprehensive FDI cyber-attack index of branch k .
$EMLDI_k$	Enhanced malicious load deviation index of line k .
$f(x)$	1 if x is positive; 0 if x is zero; -1 if x is negative.
$Indictr_{n,k}$	An indicator defining how load change at bus n would affect the flow change on branch k .
$MLDI_k$	Malicious load deviation index of branch k .
$P_{k+,SCED}$	Scheduled flow on branch k at $t = T_{ED}$, determined by SCED that runs at $t = 0$.
$w_{n,k}$	Influential factor for branch k due to change in the load at bus n .

I. INTRODUCTION

In modern power systems, energy management systems (EMSs) are used to help operators manage real-time operations. State estimation executes regularly in real-time and serves as a core function in EMS for monitoring system condition. State estimation can effectively estimate the system status with the data received from remote terminal units or local control centers through a communication network.

As many applications such as real-time contingency analysis (RTCA) and real-time security-constrained economic dispatch (RT SCED) are based on the system status determined

The research presented in this manuscript is funded by the National Science Foundation (NSF) Award (1449080).

Xingpeng Li and Kory W. Hedman are with the School of Electrical, Computer, and Energy Engineering, Arizona State University, Tempe, AZ, 85287, USA (e-mail: Xingpeng.Li@asu.edu; kwh@myuw.net).

by state estimation, it is critical to ensure the results of state estimation are correct. Traditional bad data detection and identification in state estimation can detect random bad data that are introduced by large measurement errors. It ensures the impact of random measurement noises on state estimation is minimal. However, recent work [1]-[12] in the literature shows that malicious cyber-attacks can inject false measurements that are designed to meet the physical laws and bypass bad data detection. This indicates that power system state estimation is subject to false data injection (FDI) cyber-attacks.

State estimation under FDI attack may provide a biased base case for other EMS applications. A biased system condition may mislead system operators to take incorrect actions such as improper generation adjustment, which may cause severe violations or damage to power systems. Thus, developing a detection approach that can efficiently detect FDI attacks is vital for reliability enhancements and secure operations of electric power systems.

Several metrics and an alert system are proposed in this paper to monitor abnormal load deviations and flow changes. A systematic two-stage FDI detection (FDID) approach is proposed to detect FDI cyber-attacks. Stage 1 determines whether the system is under FDI cyber-attack and stage 2 identifies the target branch. The goal of FDID is to enhance state estimation by effectively detecting FDI cyber-attacks in real-time and, thus improve system reliability. Simulation results demonstrate the effectiveness of the proposed two-stage FDID approach.

The rest of this paper is organized as follows. Section II presents a literature review on FDI and FDID. Section III and Section IV briefly explain state estimation and FDI cyber-attack respectively. Section V presents the proposed metrics, FDI alert system and systematic two-stage FDID approach. Section VI presents the FDI results and the FDID results. Finally, Section VII concludes the paper.

II. LITERATURE REVIEW

A. FDI

FDI cyber-attack on power system state estimation has gained significant attention since it was first proposed by Liu in [1] that shows FDI attacks can change the DC state estimation results in an unobservable manner. The attack model and impact are further analyzed, and more detailed results are presented in [2], as well as a generalized FDI attack.

Two regimes of attacks, a strong regime and a weak regime, are presented in [3]. The strong regime attack has access to a sufficient number of meters and can launch unobservable attacks while the weak regime attack can be detected as only a limited number of meters are under control of the attacker.

A graph theory based algorithm is proposed in [4] to identify the locations where attackers can attack with the least-number measurements to keep the attack from being detected by AC state estimation. Thus, those locations may need more protection against potential FDI attacks. It is shown in [5] that attacker can launch an unobservable attack by only introducing false measurements within a subgraph that is determined by the subgraph algorithm proposed in [4]. Extended on [5], a bi-level optimization is proposed in [6] to maximize physical flow on a target branch, which is equivalent to maximizing the branch overload. Though the FDI attack approach proposed in

[6] can cause unobservable branch overloads, it does not scale due to computation complexity. Therefore, three computationally efficient algorithms are proposed in [7] to speed-up the solution time and provide boundaries on system vulnerability. In addition, Benders' decomposition is implemented in [8] to solve FDI problems for large-scale systems in a reasonable time.

Though [5]-[8] show that the unobservable FDI attack approach can physically overload a branch, they all assume that the attacker has knowledge of the entire system. An FDI attack model with limited information is proposed in [9]. The information used in [10] is strictly limited to the attack sub-network, which is even less than the information used in [9].

As illustrated in [1]-[10], an attacker can compromise system state through an FDI attack. Moreover, the attacker can launch topology attacks. In [11], an unobservable state-preserving topology attack is investigated and an algorithm is proposed to determine the minimal attack sub-network. Built upon [11], a systematic malicious state-and-topology attack strategy is proposed in [12]. This topology attack changes both the state data and topology data of a sub-network to cover a physical topology attack and cause physical branch overloads.

B. FDID

As introduced above, [1]-[12] demonstrates that power systems are subject to unobservable FDI attacks which can cause severe physical consequences. Therefore, it is very important to develop effective approaches to detect FDI attacks.

In [13], a specific set of measurements are selected and protected in order to detect the FDI attack that is proposed in [1]. The smallest set of measurements can be determined by the proposed two approaches, brute-force search and protecting basic measurements.

It is shown in [14] that random bad data injection can be identified by state estimation while stealth bad data injection can bypass state estimation. Thus, [14] proposes a defense strategy against the stealth bad data injection by conducting real-time statistical analysis on a sequence of data at the minimum cost of delay. A least-budget defense strategy, which can achieve quality solutions in a reasonable time, is proposed in [15] to enhance state estimation against FDI attacks by protecting critical meters.

A novel FDID mechanism that uses nuclear norm minimization and low rank matrix factorization is proposed in [16] to separate the nominal power grid states and the anomalies. A real-time three-phase mechanism is proposed in [17] to detect FDI attacks by evaluating spatiotemporal correlation between system states. A centralized FDI detector that is based on the generalized likelihood ratio and a distributed FDI detector that employs the adaptive level-triggered sampling technique are proposed in [18] to efficiently detect FDI attacks.

With the assumption that the probability distributions derived from measurement variations among adjacent time steps are consistent, the cyber-attack detection approach proposed in [19] can detect most of the attacks by tracking the dynamics of measurement variations.

III. STATE ESTIMATION

State estimation processes the data received from remote terminal units (RTUs) or local control centers and estimates the system status in real-time. It provides a base case or a

starting point for other EMS functions such as RTCA and RT SCED. Thus, state estimation is an essential function of EMS as it is the basis for other modules in EMS. The sequence of power system real-time operation is illustrated in Fig. 1.

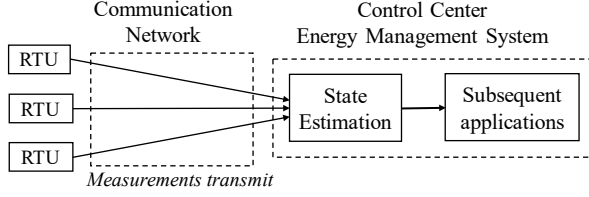


Fig. 1. Power system real-time operation sequence

State estimation is run continuously in real-time to estimate the system status, including bus voltages and branch flows. The measurement model for state estimation can be represented by (1). In (1), $h(x)$ describes the relationship between state variables x and measurements z , while e denotes the measurement error vector.

$$z = h(x) + e \quad (1)$$

For DC state estimation, the relationship between state variables x and measurements z is linear and $h(x)$ can be replaced by Hx , where H is a constant Jacobian matrix. Then, (1) can be replaced by (2) for DC state estimation. Variables x in (2) denote the bus voltage phase angles. This paper focuses on the DC model.

$$z = Hx + e \quad (2)$$

IV. FDI CYBER-ATTACK

As discussed in the previous section, it is very important to ensure state estimation works correctly as other EMS applications depend on its solution. However, prior work in literature shows that FDI cyber-attack can compromise state estimation and cause unobservable branch overloads. Fig. 2. illustrates how attackers compromise the system by replacing true measurements with false measurements.

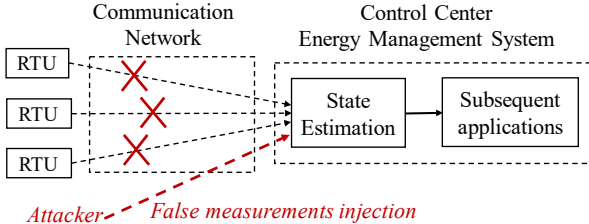


Fig. 2. Power system real-time operation under FDI cyber-attack

To launch an unobservable FDI cyber-attack, the injected false measurements should meet (3) that represents the measurement model under attack. In (3), \tilde{x} denotes the state variable under attack and \tilde{z} denotes false measurements. Equation (4) defines the relationship between the actual state variable and the cyber state variable under attack; variable c in (4) is referred to as attack vector in this paper.

$$\tilde{z} = H\tilde{x} + e \quad (3)$$

$$\tilde{x} = x + c \quad (4)$$

If the attacker has access to only a part of the system, then the measurements outside the attack area will remain the same. Thus, for the buses that are located outside the attack area, the associated elements in the attack vector c are zeros.

For simplicity, it is assumed in this work that the attacker has access to the entire system.

Fig. 3 shows the time line for illustrating the FDI cyber-attack. There are two dispatch intervals shown in Fig. 3. The assumptions made in this work are listed below:

- the attacker injects false measurements at $t = 0^-$, right before state estimation and RT SCED execute at $t = 0$,
- the dispatch point is optimal at $t = -T_{ED}$ and the generation in the first RT SCED period remain the same,
- operators have accurate information at $t = -T_{ED}$,
- state estimation executes repeatedly with the same frequency of RT SCED executions.

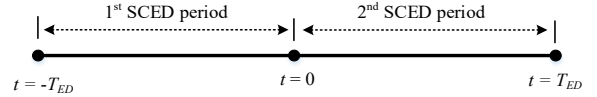


Fig. 3. Time line for illustrating the FDI cyber-attack

In [6], a bi-level optimization model is proposed to determine the attack vector and false load vector that can cause the most severe loading level on a target transmission and may result in physical flow violation. Heuristics for this bi-level model are proposed in [7] and a modified version of one of those heuristic models is presented below,

$$\text{maximize } f(P_{l,0})(p_l - \tilde{p}_l) \quad (5)$$

subject to

$$p_k = (\theta_{n(k-)} - \theta_{n(k+)})/x_k, \quad k \in K \quad (6)$$

$$\tilde{p}_k = (\tilde{\theta}_{n(k-)} - \tilde{\theta}_{n(k+)})/x_k, \quad k \in K \quad (7)$$

$$\tilde{\theta}_n = \theta_n + c_n, \quad n \in N \quad (8)$$

$$\Delta \tilde{d}_n = \sum_{k \in K(n-)} (p_k - \tilde{p}_k) - \sum_{k \in K(n+)} (p_k - \tilde{p}_k), \quad n \in NL \quad (9)$$

$$-L_S d_{n0} \leq \Delta \tilde{d}_n \leq L_S d_{n0}, \quad n \in NL \quad (10)$$

$$-c_n \leq s_n, \quad n \in N \quad (11)$$

$$c_n \leq s_n, \quad n \in N \quad (12)$$

$$\sum_n s_n \leq N_1 \quad (13)$$

The objective of this model is to maximize the difference between post-attack physical and cyber power flows on a pre-specified target branch l . Equations (6) and (7) calculate the post-attack physical branch flows and cyber branch flows respectively. Equation (8) shows the relationship between physical bus angles and cyber bus angles. Equation (9) calculates the malicious load deviation for each load bus, while (10) ensures that the load shift is within the limit. The summation of the absolute change in state variables is restricted by (11)-(13), which is equivalent to an l_1 -norm constraint [6]-[7].

The above model can be further simplified by introducing a new variable Δp_k that denotes the difference between the post-attack physical and cyber power flows. The simplified FDI cyber-attack model is formulated as follows.

$$\text{maximize } f(P_{l,0})\Delta p_l \quad (14)$$

subject to (10)-(13) and

$$\Delta p_k = (-c_{n(k-)} + c_{n(k+)})/x_k, \quad k \in K \quad (15)$$

$$\Delta \tilde{d}_n = \sum_{k \in K(n-)} (\Delta p_k) - \sum_{k \in K(n+)} (\Delta p_k), \quad n \in NL \quad (16)$$

where,

$$\Delta p_k = p_k - \tilde{p}_k, \quad k \in K \quad (17)$$

Note that this simplified $B-\Delta\theta$ FDI cyber-attack model, consisting of (10)-(17), is mathematically equivalent to the third algorithm presented in [7]. This attack model is implemented to provide data for the FDID studies in this paper.

V. FDID METHODOLOGY AND ALGORITHM

A. FDID Metrics

Two categories of metrics are proposed in this paper to effectively detect potential FDI cyber-attacks on a specific branch. They are the branch overload risk index (BORI) and the malicious load deviation index (MLDI). BORI monitors suspicious changes in branch flows and identifies potential overloads, while MLDI can recognize load change patterns and identify malicious load deviation. An FDI cyber-attack alert system is also proposed in this paper. This system has four different alert levels that are defined as *Danger*, *Warning*, *Monitor*, and *Normal*.

The proposed metrics BORI and MLDI are individual metrics for determining whether a specific branch is an attack target. Based on BORI and MLDI, systematic metrics and methodology are also proposed in this work and they are presented in Section V.B.

Branch Overload Risk Index

To execute an unobservable FDI cyber-attack that would overload a branch, the attacker can change the measurements including load measurements that are sent to the system operators. In the cyber world, the attacker can deliberately reduce the flow on a congested line or a heavily loaded line by shifting loads. This would mislead operators to believe that there is extra available capacity on the target branch; then, operators may re-dispatch generation to take advantage of that extra available capacity and reduce the total cost. However, in the real world, there is no such extra available capacity and physical overloads may occur. Thus, based on this type of flow change pattern, a branch overload risk index is proposed in this work to detect FDI cyber-attacks.

Due to the fact that attackers may or may not consider the effects of generation re-dispatch, two similar but different metrics, $BORI1_k$ and $BORI2_k$, are proposed in this paper. $BORI1_k$ only considers the flow changes in the previous interval while $BORI2_k$ takes the SCED results into account. $BORI1_k$ and $BORI2_k$ are defined in (18) and (19) respectively. A comprehensive metric $BORI_k$ is proposed to combine these two metrics. As shown in (20), $BORI_k$ is defined to be the larger value between $BORI1_k$ and $BORI2_k$.

$$BORI1_k = f(P_{k-})(P_{k-} - P_{k0,M} + P_{k-})/Limit_k \quad (18)$$

$$BORI2_k = f(P_{k-})(P_{k-} - P_{k0,M} + P_{k+,SCED})/Limit_k \quad (19)$$

$$BORI_k = \max(BORI1_k, BORI2_k) \quad (20)$$

The alert level criteria for $BORI_k$ is defined in Table I. In this table, ALB_k denotes the alert level associated with $BORI_k$ and it enables operators to determine whether a branch is under attack from the viewpoint of flow violations.

TABLE I ALERT LEVEL CRITERIA BASED ON $BORI_k$

Alert level ALB_k	$BORI_k$
<i>Danger</i>	>115%
<i>Warning</i>	>110%
<i>Monitor</i>	>105%
<i>Normal</i>	<105%

Malicious Load Deviation Index

Power transfer distribution factors (PTDF) are widely used in power system operations. They are essentially sensitivity factors that measures the incremental change in branch flow due to a change in power transferring between a slack bus and

a non-slack bus. Thus, given a branch k , the loads that have a significant impact on that branch should be monitored. It would be unusual if the changes in all the loads that are critical to branch k contribute to decreasing the flow on branch k . Therefore, based on this observation, a malicious load deviation index is proposed to detect potential FDI cyber-attacks. $MLDI_k$ is defined in (21),

$$MLDI_k = f(P_{k-}) \frac{\sum_{n \in NL(k)} Indictr_{n,k}}{NL_k} \quad (21)$$

where,

$$Indictr_{n,k} = \begin{cases} -f(PTDF_{n,k}), & \text{if } \frac{d_{no,M} - d_{n-}}{d_{n-}} \leq -5\% \\ 0, & \text{if } -5\% < \frac{d_{no,M} - d_{n-}}{d_{n-}} < 5\% \\ f(PTDF_{n,k}), & \text{if } \frac{d_{no,M} - d_{n-}}{d_{n-}} \geq 5\% \end{cases} \quad (22)$$

and

$$NL_k = \sum_{n \in NL(k)} 1 \quad (23)$$

where $NL(k)$ denotes the set of load buses that are critical to branch k . In this work, if the absolute value of $PTDF_{n,k}$ is greater than or equal to 1%, then, the associated load bus n is defined to be critical to branch k .

Though theoretically $MLDI_k$ is in the range of $[-1, 1]$, it should be close to zero if loads fluctuate randomly. A positive value indicates that the load change may decrease the flow on branch k . A very high positive value may imply the load fluctuation is abnormal and the probably of branch k being targeted by an FDI attack is high.

Metric $MLDI_k$ only considers the number of load buses that are critical to an individual branch, but it fails to take load magnitude and PTDF values into account. To consider those two factors, an enhanced malicious load deviation index ($EMLDI$) is proposed in this work. Similar to $MLDI_k$, $EMLDI_k$ is defined in (24),

$$EMLDI_k = f(P_{k-}) \sum_{n \in NL(k)} (w_{n,k} Indictr_{n,k}) \quad (24)$$

where,

$$w_{n,k} = \frac{|(d_{no,M} - d_{n-})PTDF_{n,k}|}{\sum_{n \in NL(k)} |(d_{no,M} - d_{n-})PTDF_{n,k}|} \quad (25)$$

$EMLDI_k$ shares the same range and indication with $MLDI_k$. The difference is that the effects of load magnitude and PTDF values are not considered for $MLDI_k$ but are captured by $EMLDI_k$. Thus, given a specific potential target branch k , $EMLDI_k$ may be a better indicator to determine whether there is an attack targeting that branch. The alert level criteria for $MLDI_k$ and $EMLDI_k$ are the same and are defined in Table II. As $EMLDI_k$ considers more factors than $MLDI_k$, the alert level for branch k should be determined by $EMLDI_k$. In this work, ALE_k denotes the alert level associated with $EMLDI_k$.

TABLE II ALERT LEVEL CRITERIA BASED ON $EMLDI_k$

Alert level	$MLDI_k$ or $EMLDI_k$
<i>Danger</i>	>50%
<i>Warning</i>	>35%
<i>Monitor</i>	>20%
<i>Normal</i>	<20%

B. Two-stage FDID Approach

Metrics MLDI and BORI presented in Section V.A are used to detect potential FDI attacks on a specific branch rather than to monitor the system as a whole. Thus, a systematic two-stage FDID approach, consisting of an FDI attack awareness

stage and a target branch identification stage, is proposed in this paper to detect potential FDI cyber-attacks. The first stage is to determine whether the system is under FDI cyber-attack and the second stage would identify the target branch.

Stage 1: FDI Attack Awareness

MLDI and BORI are proposed to detect whether an FDI cyber-attack is launched for a specific branch. Since system operators have limited information regarding which branch the attacker would target, it is necessary to calculate the metrics for all branches. However, given that a practical power system typically has a large number of branches, even random load fluctuations may cause large $MLDI_k$, $EMLDI_k$, and $BORI_k$ values for a few branches, which may mislead system operators to believe that the load fluctuation is abnormal and the system is under attack. Therefore, a system-wide malicious load deviation index (SMLDI) is proposed to resolve this issue. SMLDI is defined in the equation shown below,

$$SMLDI = \frac{\sum_{k \in KA} MLDI_k}{\sum_{k \in KA} 1} \quad (26)$$

where KA is a set of ten branches that have top ten $MLDI_k$ values. If the number of load buses that have significant effects on branch k is too small, then the associated $MLDI_k$ are not used for malicious load deviation recognition and branch k will not be included in the set KA . In this work, branches that have less than five critical load buses will not be considered as a candidate element of set KA .

In this stage, SMLDI is used as the metric to determine whether the system is under attack. Similar to the alert level designed for a target line, a system-wide FDI alert level is defined in Table III. A system would be considered to be FDI cyber-attack free if the associated alert level is marked as *Normal* or *Monitor* in stage 1. Only the cases that have either *Warning* or *Danger* alert flags will be sent to stage 2 for target branch identification.

TABLE III ALERT LEVEL CRITERIA BASED ON SMLDI

Alert level	SMLDI
<i>Danger</i>	>50%
<i>Warning</i>	>35%
<i>Monitor</i>	>20%
<i>Normal</i>	<20%

Stage 2: Target Branch Identification

It is vital to determine whether the system is under malicious FDI cyber-attack in stage 1. It is also very important to identify the branch that the attacker targets so that operators can take immediate actions to handle the detected FDI attack.

$EMLDI_k$ detects FDI attacks from the viewpoint of suspicious load deviations while $BORI_k$ detects FDI attacks from the viewpoint of potential flow violations. The alert level ALE_k associated with $EMLDI_k$ and the alert level ALB_k associated with $BORI_k$ can be combined into a single comprehensive FDI attack alert level, which is defined in Table IV. This comprehensive alert level, denoted by ALC_k , is used to identify the target branch.

TABLE IV DETERMINATION OF THE COMPREHENSIVE ALERT LEVEL ALC_k

ALC_k	ALE_k			
ALB_k	Normal	Monitor	Warning	Danger
Normal	<i>Normal</i>	<i>Monitor</i>	<i>Monitor</i>	<i>Warning</i>
Monitor	<i>Monitor</i>	<i>Monitor</i>	<i>Warning</i>	<i>Warning</i>
Warning	<i>Monitor</i>	<i>Warning</i>	<i>Warning</i>	<i>Danger</i>
Danger	<i>Warning</i>	<i>Warning</i>	<i>Danger</i>	<i>Danger</i>

Though the proposed alert system can provide a qualitative analysis, it is also very important to analyze the FDI attack quantitatively. Thus, a comprehensive attack index (CAI) that considers both load deviation patterns and potential branch overloads is proposed in this work. CAI_k is defined in (27). The branch that has the biggest CAI_k is considered to be the most suspicious target branch. Moreover, the CAI_k rank indicates the possibility of branch k being the target branch.

$$CAI_k = EMLDI_k BORI_k \quad (27)$$

Therefore, both the proposed comprehensive attack index CAI_k and the proposed comprehensive alert level ALC_k are used to identify the target branch in stage 2. The branches that are either marked as *Danger* or have a CAI_k ranking in the top three are considered to be the most suspicious target branches in this work.

VI. CASE STUDIES

The IEEE 118-bus test system is used in this paper to investigate the proposed FDI cyber-attack model and examine the proposed two-stage FDID approach. This case contains 118 buses, 186 branches, and 19 online units. Out of 118 buses, 99 buses are load buses. The total load at $t = -T_{ED}$ is 4,242 MW.

A. FDI Results

To study the effectiveness of the proposed FDI cyber-attack model, numerical simulations are conducted with different scenarios including constant load scenarios and random load fluctuation scenarios in the first dispatch interval. The effects of different load shift factors and l_1 -norm constraint limits on the physical consequences of an FDI attack are analyzed.

With the assumption that the load profile does not change, the maximum power flows on branch 111 and branch 118 at $t = 0$ with different FDI attack settings are presented in Fig. 4 and Fig. 5 respectively. The blue curve with diamond markers in Fig. 4 corresponds to the FDI results with a load shift factor of 5% and it becomes flat very quickly. The reason is that the load shift constraint becomes binding when N_1 increases to 6 and further relaxing the l_1 -norm constraint will not change the results. Since the $B-\Delta\theta$ FDI model proposed in this work is a fast heuristic rather than an exact approach, the maximum flows shown in Fig. 4 and Fig. 5 do not strictly increase as the load shift factor and the l_1 -norm constraint limit increases. However, with a more flexible condition, the attacker can typically cause more severe flow violations.

In reality, loads fluctuate all the time. Thus, it is important to analyze the effects of random load fluctuations on FDI cyber-attacks. It is assumed that load fluctuation follows the normal distribution with a mean of μ (a percentage) and a standard deviation of σ (a percentage), which is denoted by $N(\mu, \sigma)$. The process of generating a load fluctuation vector following $N(\mu, \sigma)$ is presented below:

- 1) generate a vector v that follows standard normal distribution,
- 2) apply a cutoff value 1.96 to this vector v ,
- 3) adjust v with equation: $v = v\sigma + \mu$,
- 4) create a load fluctuation vector: $\Delta d_n = d_n - v_n, \forall n$.

Note that since loads do not fluctuate significantly in a short-term, step 2) ensures that the random load fluctuation does not have a long tail distribution. The cutoff value 1.96 corresponds to a confidence interval of 95%.

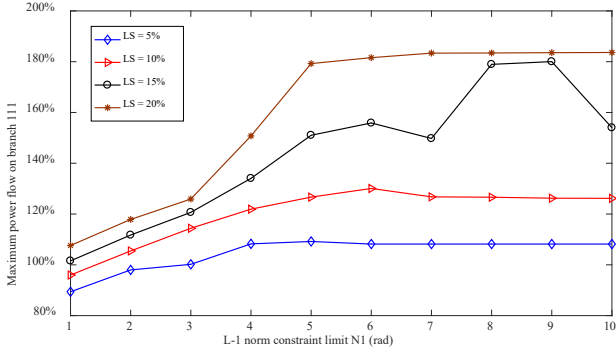


Fig. 4. Maximum power flow on branch 111 with various load shift factors and l_1 -norm constraint limits.

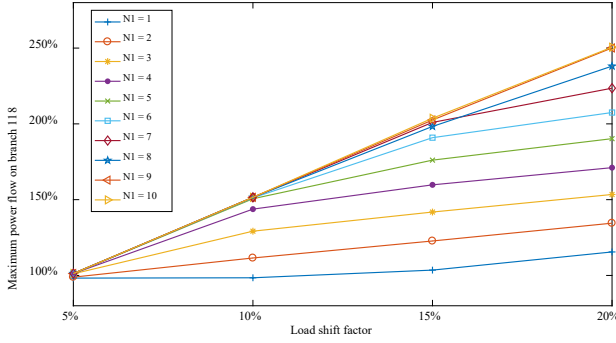


Fig. 5. Maximum power flow on branch 118 with various load shift factors and l_1 -norm constraint limits.

For the FDI simulations conducted in this section, the random load fluctuations follow the normal distribution of $N(0, 3\%)$. For each FDI attack simulated, the load profile is updated with a different randomly generated load fluctuation vector. The results of FDI attacks with load fluctuations are presented in Fig. 6 and Fig. 7. Fig. 6 shows the results of an FDI attack targeting branch 111 while Fig. 7 shows the results of an FDI attack targeting branch 118. The curves in Fig. 6 and Fig. 7 look very similar to the corresponding curves in Fig. 4 and Fig. 5 respectively. This indicates that the effects of random load fluctuations on FDI attacks are limited. Fig. 6 and Fig. 7 show that an FDI cyber-attack can still result in a flow violation on the target branch even with random load fluctuations.

B. FDID Results

Stage 1: FDI Attack Awareness

The proposed FDID strategy consists of two stages. Stage 1 determines whether the system is under an FDI cyber-attack by analyzing the load profile change pattern. It is important to detect FDI attacks while it is also vital to bypass normal random load fluctuations. The goal of stage 1 is to have a low probability of false alarm and a low probability of false dismissal. Two sets of system scenarios with different load deviation vectors, including FDI malicious load deviation vectors and random load fluctuation vectors, are tested in this stage.

The load deviation vector denotes the difference between the loads at the beginning of the second dispatch interval ($t = 0^+$) and the loads at the beginning of the first dispatch interval (at $t = -T_{ED}$). The malicious load deviation vectors are obtained from the 160 different FDI attacks performed in Section VI.A. The normal load fluctuation vectors are created with four different normal distributions: $N(0, 3\%)$, $N(0, 5\%)$, $N(-1\%$,

$3\%)$, and $N(1\%, 3\%)$. Twenty independent vectors are generated for each normal distribution and, thus the second set of system scenarios correspond to 80 load fluctuation vectors.

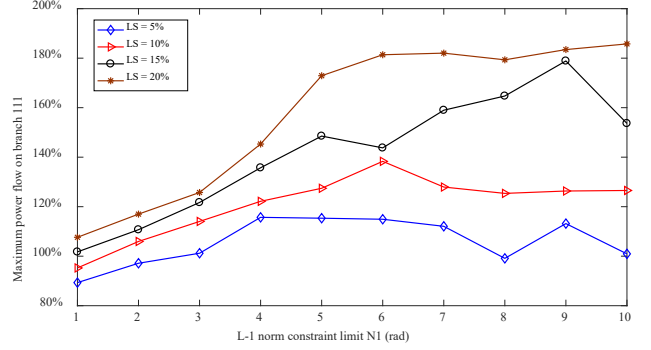


Fig. 6. Maximum power flow on branch 111 with random load fluctuation.

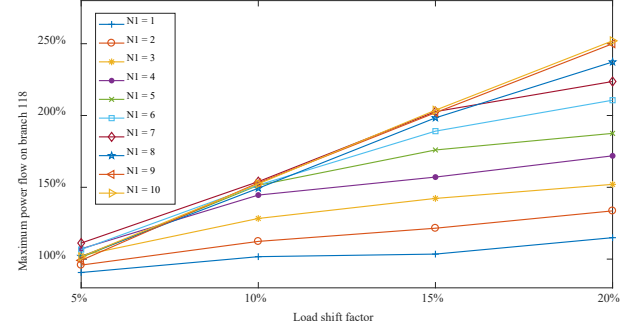


Fig. 7. Maximum power flow on branch 118 with random load fluctuation.

The SMLDI values for those 240 scenarios are calculated in stage 1. The results for the 160 FDI malicious load deviation vectors and the 80 random load fluctuation vectors are presented in Table V and Table VI respectively. The SMLDI values for the random load fluctuations are very small and the averages are close to zero. As for the FDI attacks, the associated SMLDI values are much bigger and the average values are around 70%. This indicates that FDI cyber-attacks are successfully detected with the proposed metric SMLDI and random load fluctuations can successfully bypass the proposed FDID approach.

Fig. 8 shows a scatter plot of the SMLDI values for all the random load fluctuations and FDI cyber-attacks simulated in this work. The blue squares correspond to the random load fluctuations while the red triangles correspond to the FDI cyber-attacks. As shown in Fig. 8, the SMLDI values for random load fluctuations are all below 35% and the associated alert levels are either *Normal* or *Monitor*. Moreover, the alert levels for most random vectors are *Normal*. As for the FDI cyber-attacks, the associated SMLDI values are all above the *Warning* tolerance and the alert levels for most FDI cyber-attacks are *Danger*. Therefore, it is demonstrated the proposed metric SMLDI can efficiently detect FDI cyber-attacks and would not mistakenly identify a random load fluctuation as an FDI attack. In other words, the results presented in Fig. 8 demonstrate the proposed FDID approach has a very low false alarm rate as well as a very low false dismissal rate.

The first 80 system scenarios in Fig. 8 correspond to random load fluctuations with four different normal distributions. They are listed in the order of $N(0, 3\%)$, $N(0, 5\%)$, $N(-1\%, 3\%)$, and $N(1\%, 3\%)$. Each normal distribution has 20 scenar-

ios. By comparing the random load fluctuations generated with different normal distributions, it is observed that the mean of load fluctuation does not significantly affect the metric while higher standard deviations may result in higher SMLDI values. This is consistent with the statistics presented in Table VI. This implies that the false alarm rate for the proposed approach would increase as the magnitude of load fluctuation increases. It is worth noting that loads typically do not deviate too much in a short time frame.

TABLE V SMLDI VALUES FOR FDI CYBER-ATTACKS

	Attack on branch 118		Attack on branch 111	
	Constant load	$N(0, 3\%)$	Constant load	$N(0, 3\%)$
max	97.8%	97.8%	97.8%	97.5%
min	48.8%	39.9%	35.7%	38.7%
median	62.9%	68.5%	62.9%	63.8%
average	72.1%	74.5%	68.6%	70.7%
std	16.8%	19.0%	19.4%	20.3%

TABLE VI SMLDI VALUES FOR RANDOM LOAD FLUCTUATIONS

	Normal load fluctuation and no FDI attack			
	$N(0, 3\%)$	$N(0, 5\%)$	$N(-1\%, 3\%)$	$N(1\%, 3\%)$
max	23.1%	28.0%	23.5%	20.9%
min	3.2%	13.8%	5.5%	7.5%
median	11.8%	22.8%	12.0%	12.5%
average	12.2%	21.7%	12.4%	13.2%
std	4.4%	3.7%	4.7%	3.7%

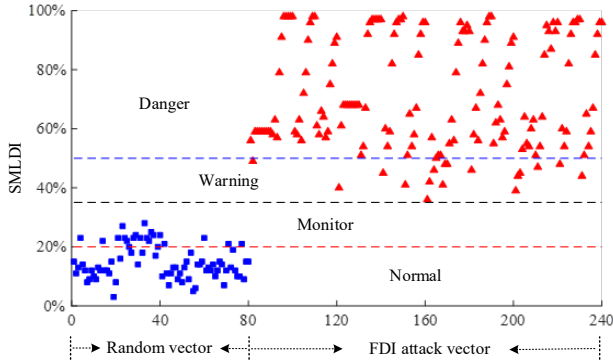


Fig. 8. SMLDI values for random load fluctuations and FDI cyber-attacks.

Fig. 9 illustrates the SMLDI values that are associated with various FDI attacks targeting branch 118 with random load fluctuations that follow $N(0, 3\%)$ in the first dispatch interval. The red dotted straight line is the boundary between the alert levels *Monitor* and *Warning*. Those SMLDI values are well above the *Warning* alert tolerance of 35%, especially for the cases that have more flexible constraints. It is very straightforward and efficient to identify whether the system is under malicious FDI cyber-attack with the proposed metric SMLDI.

Stage 2: Target Branch Identification

In stage 2, only the cases that are identified to be under FDI cyber-attack will be examined. Thus, only those 160 FDI attack scenarios identified in stage 1 are sent to the target branch identification routine.

Table VII shows the results of target branch identification against the FDI attacks on branch 111 with no random load fluctuations and a load shift factor of 10% in the FDI attack model. The metric CAI_k for branch 111 ranks first for nine scenarios out of the ten scenarios and ranks second for the remaining one scenario. There are eight scenarios for which a branch marked as *Danger* exists; and branch 111 is the only

one that is marked as *Danger* for those eight scenarios. Therefore, both the proposed comprehensive FDI attack index and the proposed comprehensive alert level successfully indicate branch 111 is the most suspicious target.

Table VIII shows the results of target branch identification against the FDI attacks on branch 111 with a random load fluctuation that follows $N(0, 3\%)$ in the first dispatch interval and a load shift factor of 10% in the FDI attack model. Thus, the simulations corresponding to Table VII do not involve random load fluctuations while the simulations for Table VIII do. Thus, the results shown in Table VIII are more realistic. However, the conclusions drawn from Table VIII are consistent with Table VII. This indicates that the proposed strategy is also very effective even when load fluctuation is considered.

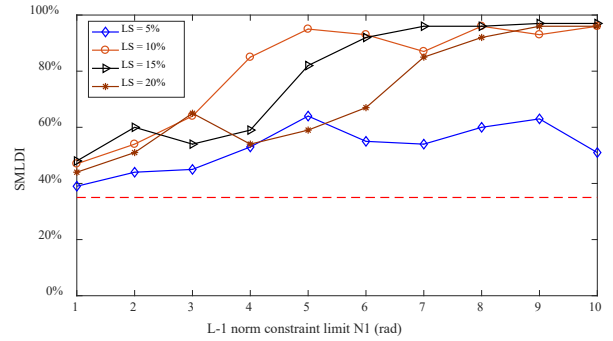
Fig. 9. SMLDI of FDI attacks targeting branch 118 with a random load fluctuation of $N(0, 3\%)$.

TABLE VII. TARGET BRANCH IDENTIFICATION RESULTS FOR FDI ATTACKS ON BRANCH 111 WITH NO RANDOM LOAD FLUCTUATIONS AND A LOAD SHIFT FACTOR OF 10% IN THE ATTACK MODEL

	CAI_{111}	Rank of CAI_{111}	ALC_{111}	Number of lines marked <i>Danger</i>
$N_l = 1$	0.46	2	<i>Monitor</i>	0
$N_l = 2$	0.66	1	<i>Warning</i>	0
$N_l = 3$	0.90	1	<i>Danger</i>	1
$N_l = 4$	1.13	1	<i>Danger</i>	1
$N_l = 5$	1.26	1	<i>Danger</i>	1
$N_l = 6$	1.30	1	<i>Danger</i>	1
$N_l = 7$	1.27	1	<i>Danger</i>	1
$N_l = 8$	1.27	1	<i>Danger</i>	1
$N_l = 9$	1.26	1	<i>Danger</i>	1
$N_l = 10$	1.26	1	<i>Danger</i>	1

TABLE VIII. TARGET BRANCH IDENTIFICATION RESULTS FOR FDI ATTACKS ON BRANCH 111 WITH $N(0, 3\%)$ RANDOM LOAD FLUCTUATION IN THE FIRST INTERVAL AND A LOAD SHIFT FACTOR OF 10% IN THE ATTACK MODEL

	CAI_{111}	Rank of CAI_{111}	ALC_{111}	Number of lines marked <i>Danger</i>
$N_l = 1$	0.45	2	<i>Monitor</i>	0
$N_l = 2$	0.68	1	<i>Warning</i>	0
$N_l = 3$	0.91	1	<i>Danger</i>	1
$N_l = 4$	1.07	1	<i>Danger</i>	1
$N_l = 5$	1.21	1	<i>Danger</i>	1
$N_l = 6$	1.37	1	<i>Danger</i>	2
$N_l = 7$	1.19	1	<i>Danger</i>	1
$N_l = 8$	1.29	1	<i>Danger</i>	2
$N_l = 9$	1.23	1	<i>Danger</i>	1
$N_l = 10$	1.20	1	<i>Danger</i>	1

Table IX presents the FDID results on various FDI attacks. As shown in this table, the target branches are correctly identified for 96.9% or 155 scenarios out of 160 FDI cyber-attacks.

The target branch is marked as *Danger* for over 90% of the FDI attacks on branch 118. The percentage of the cases that the target branch of the FDI attacks on branch 111 is marked as *Danger* is relatively low. The reason is that the overloads on branch 111 for several FDI attacks, including most FDI attacks with a load shift factor of 5%, are not very significant and do not reach the *Warning* alert threshold. However, the associated comprehensive FDI attack index of the target branch 111 ranks first for most cases. For all FDID tests on the 160 FDI attacks, the comprehensive FDI attack indices of the target branch rank very high and almost all of them rank either first or second.

TABLE IX RESULTS OF FDID ON VARIOUS FDI ATTACKS

		Average CI_k rank of the target branch	Percent of scenarios for which the target branch is identified	Percent of scenarios for which the target branch is marked as <i>Danger</i>	# of scenarios simulated
Attack on branch 118	Constant load	1.58	92.5%	92.5%	40
	$N(0, 3\%)$	1.55	100%	92.5%	40
Attack on branch 111	Constant load	1.13	100%	65%	40
	$N(0, 3\%)$	1.33	95.0%	77.5%	40
Cumulative statistics		1.39	96.9%	81.9%	160

VII. CONCLUSIONS

Recent work in the literature has demonstrated that power systems are subject to unobservable FDI cyber-attacks. Attackers can launch FDI cyber-attacks and cause overloads that are neither observed nor detected by conventional state estimation. Therefore, it is very important to develop a strategy that can quickly detect such malicious FDI cyber-attacks.

An FDI cyber-attack model is first introduced in this paper to examine the effects of FDI attacks on system reliability. Then, a two-stage strategy is proposed to detect FDI attacks. Two categories of metrics, MLDI and BORI, are proposed and used in this two-stage approach to determine whether the change in system condition is abnormal. MLDI recognizes malicious load changes while BORI identifies suspicious flow changes. In stage 1, the proposed system-wide MLDI is used to determine whether the system is under attack. If the system is deemed to be under attack, stage 2 will execute and the proposed alert system along with the proposed comprehensive FDI attack index will be used to identify the attack target branch.

Simulation results show that FDI cyber-attacks can cause physical flow violations and demonstrate the effectiveness of the proposed FDID metrics, FDI cyber-attack alert system and two-stage FDID approach. The proposed two-stage FDID approach successfully detects all 160 FDI cyber-attacks that are simulated in this work and correctly identifies the target branch for 97% of the cases. In addition, random load fluctuations will not activate the FDID alert system. Numerical simulations conducted with 80 different random load fluctuations show that none of the random load fluctuation scenarios are mistakenly identified as malicious load deviations. To conclude, normal load fluctuations will not activate the proposed FDI alert system, while the proposed two-stage FDID approach can efficiently detect FDI attacks and the target branch.

In other words, the false alarm rate and false dismissal rate for the proposed two-stage FDID approach are very low.

REFERENCES

- [1] Yao Liu, Peng Ning, and Michael K. Reiter, "False Data Injection Attacks Against State Estimation in Electric Power Grids," *Proceedings of the 16th ACM conference on Computer and communications security (CCS '09)*, Chicago, IL, USA, pp. 21-32, Nov. 2009.
- [2] Yao Liu, Peng Ning, and Michael K. Reiter, "False Data Injection Attacks Against State Estimation in Electric Power Grids," *ACM Transactions on Information and System Security (TISSEC)*, vol. 14, no. 1, Article 13, pp. 13:1-13:33, May 2011.
- [3] Oliver Kosut, Liyan Jia, Robert J. Thomas, and Lang Tong, "Malicious Data Attacks on the Smart Grid," *IEEE Transactions on Smart Grid*, vol. 2, no. 4, pp. 645-658, Dec. 2011.
- [4] Gabriela Hug and Joseph Andrew Giampapa, "Vulnerability Assessment of AC State Estimation with Respect to False Data Injection Cyber-Attacks," *IEEE Transactions on Smart Grid*, vol. 3, no. 3, pp. 1362-1370, Aug. 2012.
- [5] Jingwen Liang, Oliver Kosut, and Lalitha Sankar, "Cyber Attacks on AC State Estimation: Unobservability and Physical Consequences," *IEEE PES General Meeting*, Washington D.C., USA, pp. 1-5, Jul. 2014.
- [6] Jingwen Liang, Lalitha Sankar, and Oliver Kosut, "Vulnerability Analysis and Consequences of False Data Injection Attack on Power System State Estimation," *IEEE Transactions on Power Systems*, vol. 31, no. 5, pp. 3864-3872, Sep. 2016.
- [7] Zhigang Chu, Jiazi Zhang, Oliver Kosut, and Lalitha Sankar, "Evaluating Power System Vulnerability to False Data Injection Attacks via Scalable Optimization," *2016 IEEE International Conference on Smart Grid Communications (SmartGridComm)*, pp. 1-6, Nov. 2016.
- [8] Zhigang Chu, Jiazi Zhang, Oliver Kosut, and Lalitha Sankar, "Vulnerability Assessment of Large-scale Power Systems to False Data Injection Attacks," *arXiv preprint: 1705.04218*, May. 2017.
- [9] Jiazi Zhang, Zhigang Chu, Lalitha Sankar, and Oliver Kosut, "False Data Injection Attacks on Power System State Estimation with Limited Information," *IEEE PES General Meeting*, Boston, MA, USA, Jul. 2016.
- [10] Jiazi Zhang, Zhigang Chu, Lalitha Sankar, and Oliver Kosut, "Can Attackers with Limited Information Exploit Historical Data to Mount Successful False Data Injection Attacks on Power Systems?" *arXiv preprint: 1703.07500*, Mar. 2017.
- [11] Jiazi Zhang and Lalitha Sankar, "Implementation of Unobservable State-preserving Topology Attacks," *IEEE North American Power Symposium (NAPS)*, Charlotte, NC, USA, Oct. 2015.
- [12] Jiazi Zhang and Lalitha Sankar, "Physical System Consequences of Unobservable State-and-Topology Cyber-Physical Attacks," *IEEE Transactions on Smart Grid*, vol. 7, no. 4, Jul. 2016.
- [13] Rakesh B. Bobba, Katherine M. Rogers, Qiyan Wang, Himanshu Khurana, Klara Nahrstedt, and Thomas J. Overbye, "Detecting False Data Injection Attacks on DC State Estimation," *Proceedings of the First Workshop on Secure Control Systems*, 2010.
- [14] Yi Huang, Mohammad Esmalifalak, Huy Nguyen, Rong Zheng, Zhu Han, Husheng Li, and Lingyang Song, "Bad Data Injection in Smart Grid: Attack and Defense Mechanisms," *IEEE Communications Magazine*, vol. 51, no. 1, pp. 27-33, Jan. 2013.
- [15] Ruilong Deng, Gaoxi Xiao, and Rongxing Lu, "Defending Against False Data Injection Attacks on Power System State Estimation," *IEEE Transactions on Industrial Informatics*, vol. 13, no. 1, pp. 198-207, Feb. 2017.
- [16] Lanchao Liu, Mohammad Esmalifalak, Qifeng Ding, Valentine A. Emsih, and Zhu Han, "Detecting False Data Injection Attacks on Power Grid by Sparse Optimization," *IEEE Transactions on Smart Grid*, vol. 5, no. 2, pp. 612-621, Mar. 2014.
- [17] Po-Yu Chen, Shusen Yang, Julie A. McCann, Jie Lin, and Xinyu Yang, "Detection of False Data Injection Attacks in Smart-grid Systems," *IEEE Communications Magazine*, vol. 53, no. 2, pp. 206-213, Feb. 2015.
- [18] Shang Li, Yasin Yilmaz, and Xiaodong Wang, "Quickest Detection of False Data Injection Attack in Wide-area Smart Grids," *IEEE Transactions on Smart Grid*, vol. 6, no. 6, pp. 2725-2735, Nov. 2015.
- [19] Gu Chaojun, Panida Jirutitijaroen, and Mehul Motani, "Detecting False Data Injection Attacks in AC State Estimation," *IEEE Transactions on Smart Grid*, vol. 6, no. 5, pp. 2476-2483, Sep. 2015.